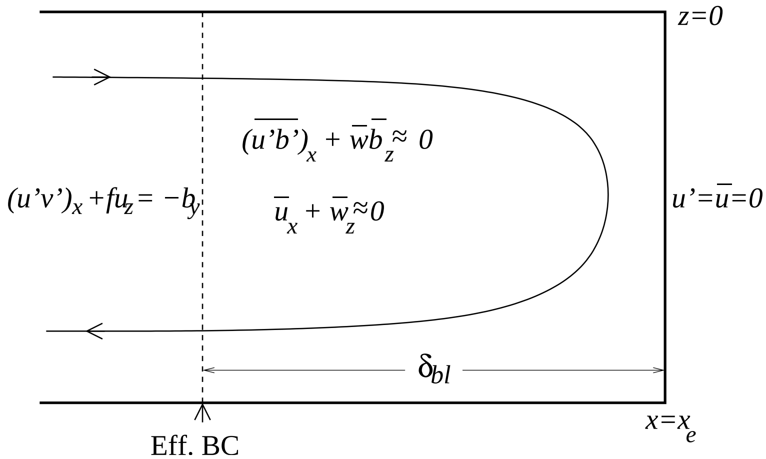

Figure 1: A sketch of the boundary layer balances and the effective boundary condition

The zonally integrated meridional volume transport of the meridional overturning circulation (MOC) is in thermal wind balance. Thus, in a basin, the MOC transport is given by the vertical integrals of the East-West difference in buoyancy, $b_e - b_w$, plus a contribution from the zonal wind stress.

A series of idealized, highly-resolved computations have shown that the contribution to the MOC from the eastern boundary, b_e, is comparable to that from the western boundary, b_w.

Model diagnostics and theoretical arguments shows that eddy fluxes of buoyancy and momentum maintain the alongshore buoyancy gradient along the eastern coast. Buoyancy eddy-fluxes arise near the eastern boundary because buoyancy gradients normal to the coast are strong. The eddy buoyancy fluxes are accompanied by mean vertical flows that take place in narrow boundary layers next to the coast where the geostrophic constraint is broken, as illustrated in figure 1.

The dynamics in these thin ageostrophic boundary layers can be replaced by *effective boundary conditions* for the interior flow, applied at the "effective coast", i.e. just at the seaward edge of the thin ageostrophic boundary layers.

This process is illustrated in figure 1 at an eastern boundary, assumed to be at $x = x_e$

Partitioning all fields in a time mean, $^{-}$, and fluctuating component, $'$, the dominant buoyancy and mass balance in the narrow up/downwelling boundary layers is illustrated in figure 1. Integrating the buoyancy balance across δ_{bl}, the "effective boundary condition" is given by

$$\left(\frac{\overline{u'b'}}{\bar{b}_z}\right)_z = \bar{u} \quad \text{or} \quad \boxed{-\bar{p}_y = \boldsymbol{\nabla}\cdot\boldsymbol{F}, \quad \text{where} \quad \boldsymbol{F} = \left(\overline{u'v'}, \overline{v'^2}, \frac{\overline{u'b'}}{\bar{b}_z}\right)},$$

The effective boundary conditions have been verified in a high-resolution ocean model.

When the *effective boundary conditions* are applied to a model of the thermocline linearized around a mean stratification, with eddy fluxes of buoyancy parametrized as isopycnal diffusion, the resulting buoyancy field model agrees very well with the time-averaged state

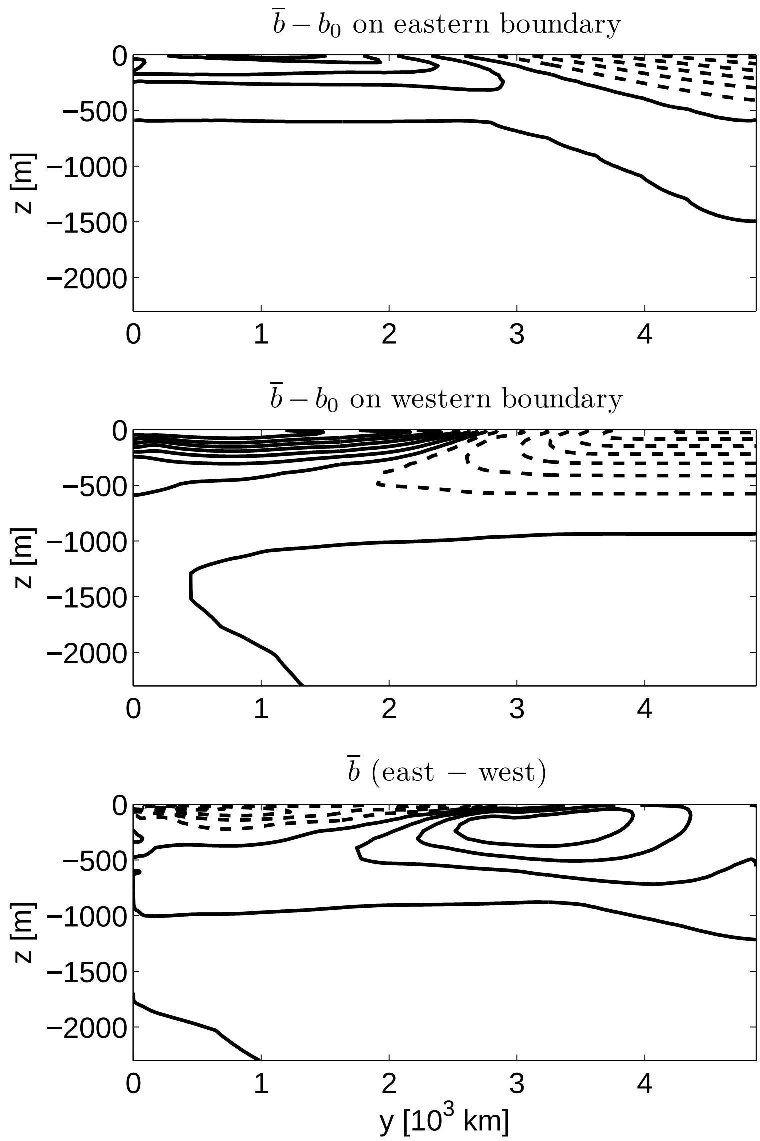

Figure 2: The time-averaged buoyancy minus the time and horizonally averaged field, $\bar{b}(x, y, z) - b_0(z)$, for an eddy-resolving computation driven by wind-stress and surface buoyancy. The top panel shows $\bar{b} - b_0$ on the eastern boundary. The middle panel shows $\bar{b} - b_0$ on the western boundary. The bottom panel is the difference between the above two fields. The vertical extent of buoyancy gradients is comparable on the two boundaries. The difference field shows two overturning cells: a shallow, thermally indirect cell in the subtropics and a deeper, thermally direct cell centered in the subpolar gyre. The contour interval for all three panels is $2 \times 10^{-3} m\, s^{-2}$. Negative values are dashed.

of an eddy-resolving computation.

In conclusion, the buoyancy and pressure gradient on the eastern boundary is maintained by eddy fluxes of buoyancy and momentum, and it is comparable to its western counterpart. Thus, the variability on the eastern boundary, due to wind and buoyancy fluctuations, will contribute to the variability of the MOC as much as the western boundary.